Dynamics of Barkhausen jumps in disordered ferromagnets

Guang-Ping Zheng[a] and Mo Li
School of Materials Science and Engineering, Georgia Institute of Technology, 771 Ferst Drive. N.W., Atlanta, Georgia 30332

Jinxiu Zhang
Department of Physics, Zhongshan University, 135 Xin Gan Road, Guangzhou 510275, China

(Received 28 January 2002; accepted for publication 1 May 2002)

Evolution of Barkhausen jumps during the magnetization reversal process in disordered magnetic material is investigated. Based on the magnetoelastic effect (ΔE effect), we investigated the dynamics of Barkhausen jumps through an internal friction measurement of amorphous Fe–B–Mo ribbons. The ΔE caused by the Barkhausen jump is found to have a power-law scaling relation with the driving rate of magnetic field. Using numerical simulation, dynamics of Barkhausen avalanches in a realistic spin-lattice model for a disordered ferromagnet is analyzed. The dynamic scaling and inhomogeneous behavior observed in both experiments and theoretical models are presented and discussed. © *2002 American Institute of Physics.* [DOI: 10.1063/1.1488249]

I. INTRODUCTION

It is known that disorder in ferromagnets causes anisotropy and Barkhausen jumps in magnetization curves.[1–5] The magnetic Barkhausen noise is sensitive to domain-wall pinning configuration which is affected by a domain or multidomain structure, grain size, and residual stress. The Barkhausen effect plays an important role in determining the microstructure properties of magnetic materials and the quality of magnetic recording and data storage materials.[6,7] In the magnetic storage industry, Barkhausen noise is a major concern in design and fabrication of thin-film inductive readers and magnetoresistive heads. For example, in a thin-film inductive head made of soft magnetic materials, Barkhausen noises usually occur after a write or erase operation. The duration time of Barkhausen jumps varies widely ranging from a nanosecond to a millisecond. As recent developments[8] of computer technology require the magnetic hard disk drive to operate in ultrahigh frequency, the Barkhausen noise can play a significant role in current magnetic recording materials. Consequently, many efforts are made to reduce or eliminate Barkhausen noise. Better understanding of the dynamic process of Barkhausen jumps in magnetic recording materials can, therefore, be very useful in the development of novel technology for future ultrahigh density and high data rate recording.[9]

Barkhausen noise is caused by movement of magnetic domains or avalanches. These domains evolve collectively, exhibiting nonequilibrium collective behavior in the system driven far from equilibrium. Although the Barkhausen signal manifests as a random process in space and time domains, in many disordered ferromagnets, the distribution of Barkhausen jumps in magnetic hysteresis loop exhibits statistical scaling behaviors. It is interesting to notice that the scaling exponents are related to the critical exponents of disorder-driven phase transitions in the system without applied field.[10,11] As for equilibrium systems, the scaling relations obtained from the magnetization reversal systems could shed a great deal of light on our understanding of the nonequilibrium phase transitions.

Most of the experimental[5,6] and theoretical[10,11] work on Barkhausen avalanches in disordered ferromagnets have focused on their stationary or metastable behaviors, e.g., the statistical distribution of signal strength and duration time of Barkhausen noises. There is little knowledge about the dynamical properties of Barkhausen avalanches.[12,13] For example, how avalanches evolve and how the driving rate of an applied field affects the avalanche kinetics[13] remain unknown. The question concerning the nature of the dynamics of the Barkhausen avalanche process, especially whether this process is homogeneous or heterogeneous, has not been clear.

The major motivation for this work is to provide some detailed understanding of the dynamic Barkhausen process through experiment and simulation studies. In Sec. II a new experimental technique using the magnetoelastic effect is developed to measure the rate-dependent Barkhausen jumps in soft magnetic materials. In Sec. III a realistic model for Barkhausen jumps is analyzed using Monte Carlo simulation and the dynamic scaling is obtained.

II. MEASUREMENT OF BARKHAUSEN DYNAMICS VIA THE ΔE EFFECT

A. Experimental method and procedure

Most of the experimental investigations[2,6] of Barkhausen noise are based on measurements of the induced flux generated by the Barkhausen jumps. However, kinetics of Barkhausen jumps may not be characterized well by the inductive method. An alternative, and more accurate, approach is to measure the built-in changes in the sample resulting from the Barkhausen jumps. For example, the magnetoelastic effect can cause a large change in the Young's modulus of amorphous magnets.[14] This change can be readily monitored with high accuracy using vibrating-reed internal friction measurements.

[a]Electronic mail: gz15@mail.gatech.edu

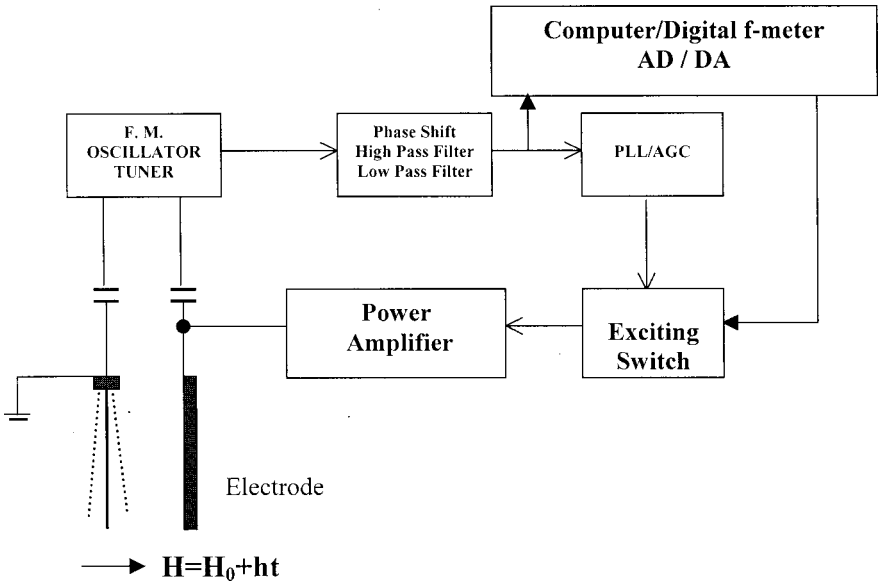

FIG. 1. Automatic vibrating-reed apparatus for ΔE measurement. The sample is placed in a solenoid.

It is well known that Barkhausen jumps are caused by the avalanches of local magnetic domains and strongly depend on the varying rate of an external field. These rate-dependent properties suggest that we could study the dynamics of Barkhausen jumps in experiment through the measurement of the dynamic response of ferromagnets. One such approach could be accomplished by measurement of the ΔE effect:[3,4] Due to magnetostriction, magnetization coupling to the mechanical degrees of freedom of the system can lead to large changes in elastic properties such as Young's modulus in ferromagnet alloys. In iron-based amorphous alloys, the ΔE effect could be very large such that the determination of dynamics of Barkhausen avalanches is possible. In this work we measure the ΔE effect on Fe–Si–Mo metallic glass ribbon using the vibration-reed technique.

The samples of Fe–Si–Mo amorphous ribbons are prepared by the melt-spinning method. The nominal composition is $Fe_{86.15}Si_{10.56}Mo_{3.29}$ as analyzed by electron dipersive x-rays analysis (EDAX). The thickness of the ribbon is about 0.04 mm. The ribbon is cut into 5×15 mm^2 sized specimens. The specimens are then annealed at 370 °C in the furnace at Ar-atmosphere for 20 min to relieve residual stress. The crystallization temperature of these samples is around 480 °C. The x-ray diffraction pattern shows that the specimens are amorphous before and after annealing. Soft magnetic properties of these magnetic glasses were measured using the induction method. The coercive force is less than 8 A/m. The addition of Mo reduces the saturation magnetization compared with Fe–Si–B magnetic glasses.

The schematic of the experiment device is illustrated in Fig. 1. The specimen is fixed as a cantilever beam and forms a part of the parallel plate capacitor, together with a fixed-drive plate made of copper. The resonant frequency can be changed through adjusting the length of the cantilever beam. The internal friction and Young's modulus (or the square of vibrating frequency) are measured using this vibrating-reed technique. To activate the vibration of a specimen, a dc voltage is applied to the capacitor. Using phase-locked-loop control,[15] the dc voltage is adjusted by the power-amplifier unit to maintain the vibration with fixed amplitude. This apparatus allows us to automatically measure the vibrating frequency in the range of 100 Hz–20 kHz. For the metallic glass ribbon, the dc voltage is typically several hundred volts and the results of internal friction and Young's modulus are independent of the dc voltage.

The accuracy for the relative change of Young's modulus $\Delta E/E_r$, where E_r is the Young's modulus without applied magnetic field, is in the order of 10^{-5}. The accuracy for the internal friction (Q^{-1}) is 10^{-5}. The magnetic field, which is generated by a coil solenoid, is maintained to be a linear-increased field at very low varying rate ($h=10^{-4}-10^{-1}$ A/ms^{-1}). This linear varying field can be obtained by connecting the coil solenoid to a generator whose output current is in sawtooth wave form. The magnetic field is applied perpendicular to the ribbon. Before each measurement, the magnetic field inside the solenoid is calibrated using a Hall sensor near the specimen surface. After the calibration the strength of the magnetic field imposed on the ribbon can be read from a current meter. The measurements were made at room temperature. ac (50 Hz) magnetic fields were used for demagnetization after each measurement.

B. Results

Typical dynamic behavior of Barkhausen jumps can be seen from time-dependent measurements of internal friction and Young's modulus, as shown in Fig. 2. The applied magnetic field is kept as a constant and the internal friction and Young's modulus are measured every 0.05 s. The magnetic domains first show smooth relaxation and then come to Barkhausen jumps manifested as several abrupt changes in the internal friction and Young's modulus.

To investigate the kinetics of a Barkhausen avalanche, a linear varying magnetic field is applied. Under large magnetic field, the ΔE increases with increasing magnetic field, i.e., normal magnetoelastic effect in a transverse domain structure. Since the coercive force is small in the metallic glass specimen, large Barkhausen jumps emerge when the

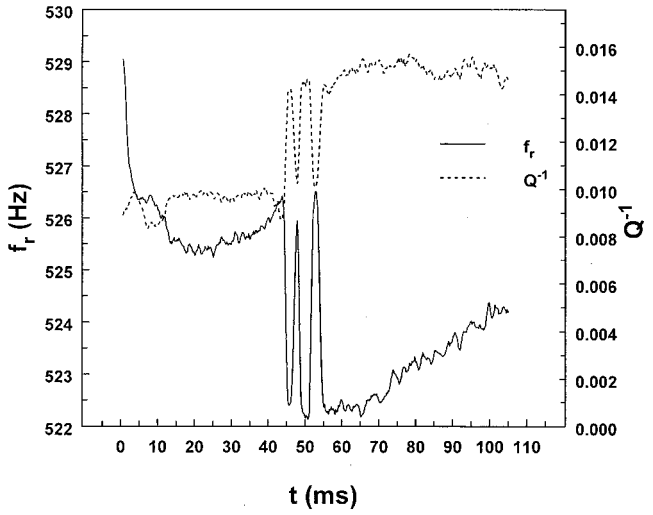

FIG. 2. The time-dependent resonant frequency and internal friction. $H=0$ when $t<0$. At $t\geqslant 0$, the magnetic field is maintained at $H=4.0$ A/m.

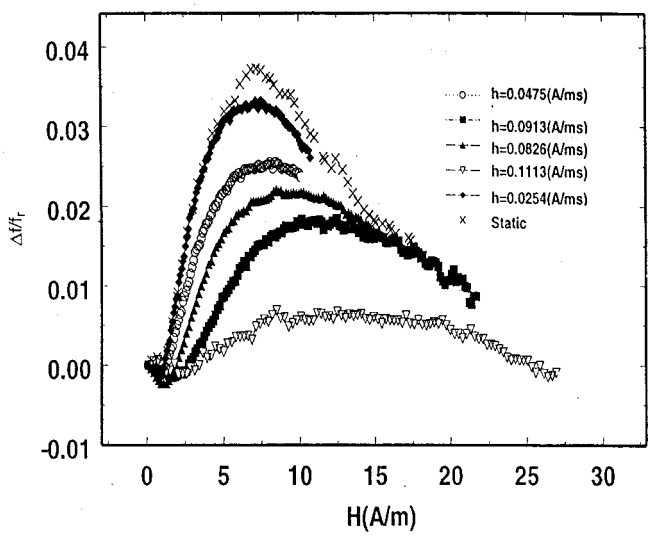

FIG. 4. The effect of field varying rate h on the ΔE effect in amorphous Fe–Si–Mo. $f_r=323.1$ Hz.

magnetic field is increased to around 2 A/m. Figure 3 shows the dependence of ΔE on the applied field and the effect of the driving rate on the ΔE effect in the low field region. The vibrating frequency at $H=0$ is $f_r=7.98$ kHz and the Young's modulus is $E_r \propto f_r^2$. The peak of the $\Delta E/E_r \sim H$ curve indicates the emergence of the largest Barkhausen avalanche. This peak shifts to a higher magnetic field if the varying rate of the magnetic field increases. Figure 4 shows the ΔE effects in the specimen with vibrating frequency $f_r=323.1$ Hz.

We can determine the maximum height e_m of the $\Delta E/E_r \sim H$ curve at different driving rates and calculate $\Delta E_m = e_0 - e_m$, where e_0 is the maximum height of the $\Delta E/E_r \sim H$ curve at static driving field. Figure 5 shows the relation between ΔE_m and h. It can be seen that $\Delta E_m \sim h$ curves have power-law relations if the driving rates h are small:

$$\Delta E_m \equiv e_0 - e_m \propto h^{\alpha}. \tag{1}$$

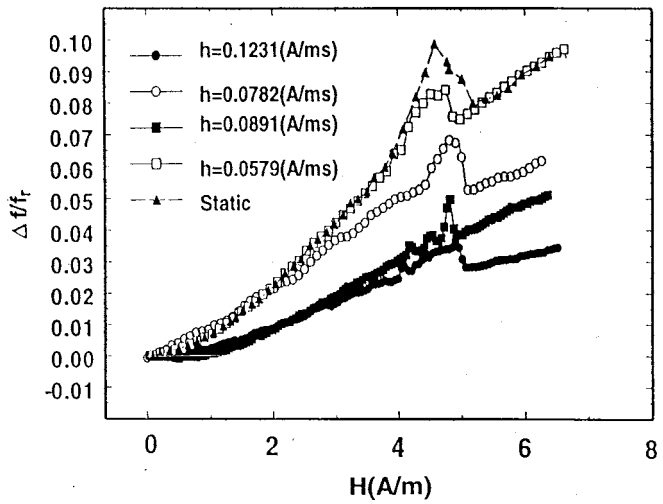

FIG. 3. The effect of field varying rate h on the ΔE effect in amorphous Fe–Si–Mo. At room temperature, the resonant frequency without magnetic field is $f_r=7.98$ kHz.

The exponent α is not affected by the vibrating frequency of the specimen.

The relation between ΔE_m and h indicates that the dynamics of Barkhausen avalanches is affected by the field driving rates. Because its scaling exponent does not change with the vibrating frequency, the power-law relation between ΔE_m and h may serve as a new scaling relation to the dynamics of Barkhausen jumps in the amorphous ferromagnet. Therefore the ΔE effect is a useful property for investigation of the short-time evolution of Barkhausen avalanches.

III. DYNAMICS OF BARKHAUSEN JUMPS IN A MODEL SYSTEM

A. A random-field Ising model for Barkhausen jumps

To consider the Barkhausen jumps in the disordered magnetic system, we employed a coarse-grained Ising model with quenched-in disorder. This model corresponds to a simplified random anisotropy model in the case of infinite an-

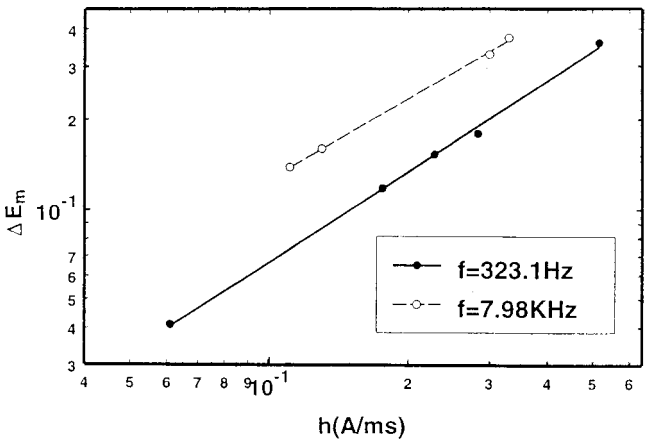

FIG. 5. The log-log plot of the relation between ΔE_m and h.

isotropy, which describes the magnetic properties of an amorphous ferromagnet well. The Hamiltonian of a three-dimensional system is written as

$$\hat{H} = -\sum_{\langle ij \rangle} J_{ij} S_i S_j - \sum_i h_i S_i - H \sum_i S_i, \tag{2}$$

where S_i ($+1$ or -1) is the spin variable at cubic lattice site i and $\langle ij \rangle$ denotes the summation extending over all nearest-neighbor spins. The exchange interaction J_{ij} between nearest-neighbor spins is a constant J. H is a homogeneous external magnetic field; h_i is an uncorrelated random field that simulates the effect of disorder on the spins. The random fields have Gaussian distribution with zero mean and variance D^2. H and D are in units of J.

The system described by Eq. (2) has been investigated extensively in the past. The critical temperature T_c for a paramagnetic–ferromagnetic phase transition decreases to zero as D increases to $D_c = 2.16$ in a three-dimensional (3D) system. For strong disorder the system may be trapped in metastable states if the magnetic field is not applied. Thermal fluctuation is too small to activate the system from those metastable states in finite time scales. Therefore to investigate the evolution of Barkhausen jumps under a fast varying applied field, we keep the temperature T of the system at zero.

At $T=0$, the system described by Eq. (2) shows a disorder-driven phase transition at $D=D_c$. Under a sweeping magnetic field at $D \geqslant D_c$, there are only small Barkhausen jumps in the hysteresis loop; while at $D<D_c$, there exists an abrupt change in the magnetization curve. The critical scaling for the disorder-driven phase transition has the following relations:[10]

$$\Delta M \sim (D_c - D)^{\beta\nu}, \qquad \langle t_0 \rangle \sim (D_c - D)^{-\nu z}, \tag{3}$$

where ΔM and $\langle t_0 \rangle$ are the largest Barkhausen jump and its duration time during a magnetization reversal process, respectively. β, ν, and z are critical exponents that characterize the phase transition at $D=D_c$. Moreover, the equilibrium distributions of all Barkhausen jumps are found to obey the power-law scaling relations at $D=D_c$,[10,11]

$$P(s) \sim s^{-a}, \qquad P(\tau_0) \sim \tau_0^{-b}, \qquad A(f) \sim f^{-c}, \tag{4}$$

where s and τ_0 are avalanche size and duration time, respectively. $A(f)$ is the power spectral density of the Barkhausen signal. a, b, and c are scaling exponents related to the critical exponents of the system.

Equations (3) and (4) are the results obtained from stationary or metastable scaling, i.e., the scaling relation is analyzed when the Barkhausen avalanches remain unchanged or metastable. We are interested in the nonequilibrium dynamic behavior of a Barkhausen avalanche in this model system.

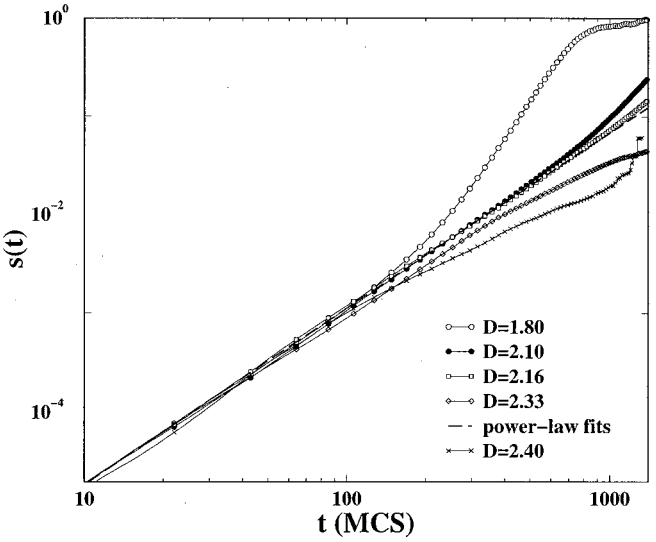

FIG. 6. Evolution of the largest Barkhausen avalanche at different disorder strengths in a 3D RFIM. The dashed line is the best power-law fit. The plots are in log-log scales. The system size is $L=128$.

B. Dynamic scaling for Barkhausen avalanches

Monte Carlo simulations are used for the numerical study of the 3D random field Ising model (RFIM). The algorithms used are described below: For the systems governed by Eq. (2), all spins are updated simultaneously. A spin will flip if its local field $f_i = \Sigma J_{ij} S_j + h_i + H$ changes sign. The external field is decreased by dH and then is fixed to drive the Barkhausen avalanches until the system reaches a metastable state. The time-dependent avalanche size is calculated from the expression $s(t) = [m(t) - m(0)]/2$, where $m(t)$ is the magnetization at time t. One time step, or one Monte Carlo step (MCS), in the simulation is defined as one attempt of all spin update. When the driving field changes, the time is reset to zero. The varying rate of magnetic field can be measured by dH. If dH is fixed throughout the magnetization reversal process, H is a linear varying field. If dH is adjusted to be the local field of the most unstable spin, H is a quasi-static driving field. To speed up the simulation, a fast algorithm similar to the sort-list algorithm[11] is used. Physical quantities are averaged over at least 5000 random field configurations. The system has 128^3 spins.

The evolution of the largest Barkhausen jump is monitored at different disorder strengths D. Figure 6 shows the evolution of the largest Barkhausen jumps under an infinite slow driving field. The short-time evolution can be fitted to a power law in time. At $D=D_c$, because the duration time of the largest Barkhausen jump tends to infinity in a large system, the power-law dynamic scaling can be well obtained as

$$\langle s(t) \rangle \sim t^{[d-\beta/\nu]/z} \sim t^{\theta}, \tag{5}$$

where $d=3$ is the dimensionality and $\theta = 1.76 \pm 0.02$ is a new exponent that characterizes the Barkhausen avalanche. $\langle\ \rangle$ denotes the average over random fuild configuration. In Eq. (5), the relation among exponents θ, β/ν, and z can be checked by using the exponents β, ν, and z determined from simulation[11] and theoretical studies[16] that are based on the stationary scaling [Eqs. (3) and (4)]. We find that $\theta = [d - \beta/\nu]/z$ holds well.

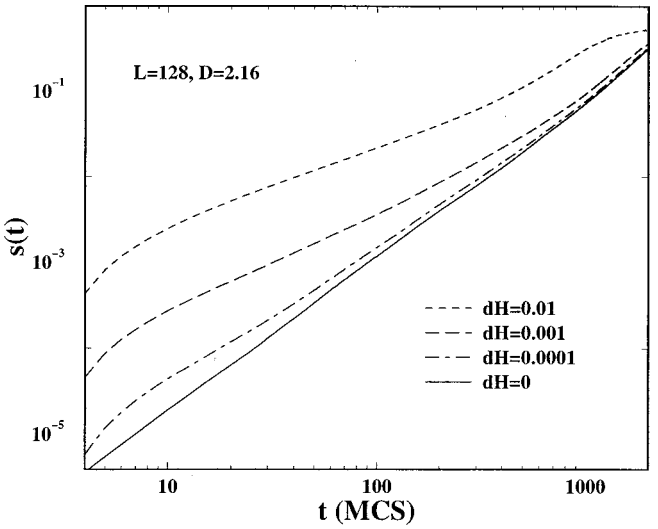

FIG. 7. The effect of varying rate dH on the evolution of the largest avalanche in a 3D RFIM. $dH=0$ denotes the quasi-static driving. The plots are in log-log scales.

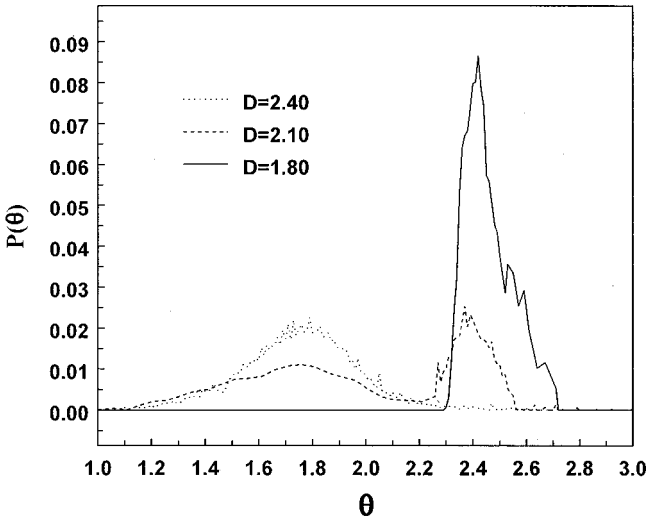

FIG. 8. The histogram plot of the distribution of exponent θ at different strengths of disorder in 3D RFIM. The system size is $L=128$.

The driving rate of applied field can be changed by adjusting dH. Figure 7 shows the effect of driving rate on the kinetics of the largest avalanche at $D=D_c$. The driving rate has a strong impact on the Barkhausen jump in short times. At the late stage, the evolution is independent of driving rate. In short times, the larger the driving rate, the faster the largest Barkhausen jump evolves.

Besides the largest Barkhausen avalanche, there are many small avalanches in the magnetization reversal. To analyze the kinetics of all these Barkhausen jumps, we measure the characteristic exponent θ defined as

$$\theta=\frac{\log s_2-\log s_1}{\log \Delta t}, \tag{6}$$

where $\Delta t=t_2-t_1$. s_2 and s_1 are the size of Barkhausen jumps at time t_2 and t_1, respectively, in an avalanche process. $t_1=4$ MCS and t_2 is taken to be $4\tau_0/5$. The distribution of this characteristic exponent is plotted in Fig. 8. When $D \geqslant D_c$, there is only one peak in the histogram plot. The peak position is near the value of exponent ($\theta=1.76$) in Eq. (5), i.e., the scaling exponent for the largest Barkhausen jump. When $D<D_c$, there is another peak at $\theta'=2.30$. The histogram plot of Eq. (6) suggests two important features of the kinetics of Barkhausen jumps. First, all Barkhausen avalanches grow with power law in times at the initial stage of evolution. The exponents are characterized by $\theta=1.76$. Second, when the disorder strength D is slightly below D_c, the Barkhausen jumps are dynamically heterogeneous, i.e., there are two distinct processes that governed the kinetic of large Barkhausen jumps.

IV. DISCUSSIONS AND CONCLUSIONS

The relation between ΔE effect and the permeability μ can be written as $\Delta E/E \propto \mu$.[17] In this study, μ (h,t) can be defined as a dynamical permeability if the magnetic field is a linear driving field. Therefore the abrupt Barkhausen jump in the magnetization reversal process gives rise to a large ΔE effect. Since the dynamical permeability usually decreases with increasing driving rate, the maximum of the relative change ΔE_m increases with increasing driving rate, as observed in our measurements.

In the RFIM for Barkhausen jumps, the driving-rate-dependent Barkhausen jumps suggest that the higher the driving rate the slower the Barkhausen avalanches evolve. Therefore the dynamical permeability is small under a high-frequency sweeping field and the Barkhausen jump is less significant. The simulation results are consistent with the experiments. These features are very important to the design of the magnetic head and media used for the high-data-rate recording.

To summarize, the dynamics of a Barkhausen avalanche is analyzed through an internal friction measurement of the ΔE effect. A vibrating-reed device is built to measure the subtle change of the vibrating frequency caused by the Barkhausen jumps. This technique is found to be of high resolution for the measurement of a dynamic Barkhausen jump. The responses of Barkhausen jumps under a linear driving field are investigated. The discontinuity of the Young's modulus is observed when the largest Barkhausen jump occurs. The related change of the Young's modulus (ΔE_m) due to the largest Barkhausen jump is found to show power-law scaling relation with respect to the driving rate when the driving rate h is small: $\Delta E_m \propto h^{\alpha}$. This power-law scaling and the scaling exponent α is independent of the vibrating frequency in the measurement. A random-field Ising model for the Barkhausen avalanches is employed for the simulation investigation on the dynamics. The kinetics of the largest Barkhausen jump is found to follow a power law in short times. The scaling exponent of this power-law relation is $\theta=1.76$, which reflects the dynamical nature of the magnetization reversal process in the disordered ferromagnet. Besides the kinetics of the largest Barkhausen jump, the evolutions of other Barkhausen avalanches in the magnetization process are also characterized. The kinetics of Barkhausen jumps shows two distinct dynamical processes.

Although the kinetics is inhomogeneous in nature, all Barkhausen jumps are observed to have the same power-law evolution in short times.

ACKNOWLEDGMENT

G. P. Z. and M. L. are grateful for the support provided by the U.S. DOE Contract No. (DE-FG02-99ER45784).

[1] A. Vazquez and O. Sotolongo-Costa, Phys. Rev. Lett. **84**, 1316 (2000).
[2] D. Spasojevic, S. Bukvic, S. Milosevic, and H. E. Stanley, Phys. Rev. E **54**, 2531 (1996).
[3] K. Moorjani, *Magnetic Glass* (Elsevier, Amsterdam, 1984).
[4] *Amorphous Metallic Alloys* edited by F. E. Luborsky (Buttermonths, London, 1988).
[5] G. Durin and S. Zapperi, Phys. Rev. Lett. **84**, 4705 (2000); P. J. Cote and L. V. Meisel, *ibid.* **67**, 1334 (1991); L. V. Meisel and P. J. Cote, Phys. Rev. B **46**, 10822 (1992).
[6] R. J. Lopez, Rev. Sci. Instrum. **70**, 171 (1999).
[7] K. B. Klaassen and J. C. L. Vanpeppen, IEEE Trans. Magn. **26**, 1697 (1990).
[8] J. H. Judy, J. Magn. Magn. Mater. **235**, 235 (2001).
[9] K. B. Klaassen, R. G. Hirko, and J. T. Contreras, IEEE Trans. Magn. **34**, 1822 (1998).
[10] E. Vives and A. Planes, Phys. Rev. B **50**, 3839 (1994); R. E. Vives, J. Goicoechea, J. Ortin, and A. Planes, Phys. Rev. E **52**, R5 (1995).
[11] J.-C. Angles D'Auriae and N. Sourlas, Europhys. Lett. **39**, 473 (1997); O. Perkovic, K. A. Dahmen, and J. P. Sethna, Phys. Rev. B **59**, 6106 (1999); Phys. Rev. Lett. **75**, 4528 (1995).
[12] B. Tadic, Phys. Rev. Lett. **77**, 3843 (1996); Physica A **270**, 125 (1999); B. Tadic and V. Nowak, Phys. Rev. E **61**, 4610 (2000).
[13] G. Bertotti, G. Durin, and A. Magni, J. Appl. Phys. **75**, 5409 (1994).
[14] P. T. Squire, J. Magn. Magn. Mater. **160**, 11 (1999).
[15] H. M. Simpson and A. Sosin, Rev. Sci. Instrum. **48**, 1392 (1972).
[16] I. Dayan, M. Schwartz, and A. P. Young, J. Phys. A **26**, 3093 (1993).
[17] M. Kersten, Z. Phys. **85**, 708 (1933).